PAPER

A theoretical study on the formation and oxidation mechanism of hydroxyalkylsulfonate in the atmospheric aqueous phase

Danna Zhang, [ID][a] Guochun Lv,[a] Xiaomin Sun,*[a] Chenxi Zhang [ID][b] and Zhiqiang Li*[c]

Hydroxymethanesulfonate (HMS) is an important organosulfur compound in the atmosphere. In this work, we studied the formation mechanism of HMS *via* the reaction of formaldehyde with dissolved SO_2 using the quantum chemistry calculations. The results show that the barrier (9.7 kcal mol^{-1}) of the $HCHO + HSO_3^-$ reaction is higher than that (1.6 kcal mol^{-1}) of the $HCHO + SO_3^{2-}$ reaction, indicating that the $HCHO + SO_3^{2-}$ reaction is easier to occur. For comparison, the reaction of acetaldehyde with dissolved SO_2 also was discussed. The barriers for the $CH_3CHO + HSO_3^-$ reaction and $CH_3CHO + SO_3^{2-}$ reaction are 16.6 kcal mol^{-1}, 2.5 kcal mol^{-1}, respectively. This result suggests that the reactivity of HCHO with dissolved SO_2 is higher than that of CH_3CHO. The further oxidation of $CH_2(OH)SO_3^-$ and $CH_3CH(OH)SO_3^-$ by an OH radical and O_2 shows that the $SO_5^{\cdot-}$ radical can be produced.
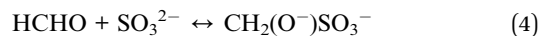
Introduction

Organosulfur compounds (OS), including organosulfates ($ROSO_3^-$), sulfones (RSO_2R'), and sulfonates (RSO_3^-),[1,2] have been identified to widely exist in fog, rainwater and in ambient atmosphere aerosols.[3–6] These OS can be produced from marine sources including dimethylsulfide (DMS) emissions and oxidation of primary marine biomass,[7,8] and their formation can be affected by aerosol acidity, relative humidity and concentration of nitrogen oxides (NO_x).[3,9,10] Hydroxymethanesulfonate (HMS) is one of the important organosulfur compounds and is a significant contributor to secondary aerosol formation.[6] The other hydroxyalkylsulfonate species are considered to be less important than HMS.[11] HMS has been misidentified as inorganic sulfate (SO_4^{2-}) for a long time, which results in discrepancies between sulfate observation and model results. As a matter of fact, HMS is an important OS compound, and it may account for about 1/3 of the missing sulfate in Beijing winter haze aerosols.[12]

The formation of HMS has been studied by many researchers. The reaction between SO_2 and HCHO contributes to its formation. Wagner *et al.* proposed that the reaction rate was determined by both HSO_3^- and SO_3^{2-} ($HCHO + HSO_3^- \rightarrow CH_2(OH)SO_3^-$; $H_2O + HCHO + SO_3^{2-} \rightarrow CH_2(OH)SO_3^- + OH^-$).[13] But in subsequent study, Peter *et al.* disagreed with Wagner's conclusion and thought that termolecular process

($H_2O + HCHO + SO_3^{2-} \rightarrow CH_2(OH)SO_3^- + OH^-$) was impossible, and the kinetics should be explained by such reactions: $HCHO + HSO_3^- \rightarrow CH_2(OH)SO_3^-$; $HSO_3^- \leftrightarrow SO_3^{2-} + H^+$. They believed that only HSO_3^- could react with HCHO and determine the reaction rate.[14] However, the experiment using spectrophotometer showed that the SO_3^{2-} reacts rapidly with HCHO.[15] In the spectrophotometric study on the reaction between dissolved SO_2 and HCHO, it can be concluded that HSO_3^- and SO_3^{2-} can react with HCHO, and the rate for SO_3^{2-} is higher than HSO_3^- obviously.[16] In a recent research, the important organosulfur compound (HMS) was been investigated for its important role in haze aerosols.[12] And this paper proposed a potentially HMS chemical mechanism. According to the analysis above, the chemical formation of HMS can be illustrated as:[16,17]

$$SO_2 \cdot H_2O \leftrightarrow HSO_3^- + H^+ \tag{1}$$

$$HSO_3^- \leftrightarrow SO_3^{2-} + H^+ \tag{2}$$

$$HCHO + HSO_3^- \leftrightarrow CH_2(OH)SO_3^- \tag{3}$$

$$HCHO + SO_3^{2-} \leftrightarrow CH_2(O^-)SO_3^- \tag{4}$$

$$CH_2(OH)SO_3^- \leftrightarrow CH_2(O^-)SO_3^- + H^+ \tag{5}$$

$$CH_2(OH)SO_3H \leftrightarrow CH_2(OH)SO_3^- + H^+ \tag{6}$$
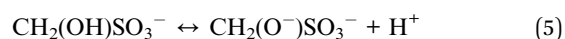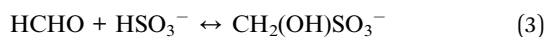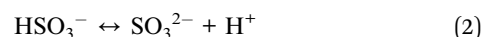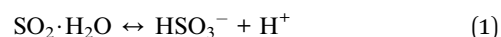
Although the HMS formation mechanism has been proposed in many researches, there is no theoretical calculation on it. Thus, in order to confirm whether the mechanism is reliable, theoretical calculation is necessary to be done.

In this paper, we investigated the reaction HCHO with HSO_3^- and SO_3^{2-} using quantum chemical calculations. In

[a]Environment Research Institute, Shandong University, Jinan 250100, China. E-mail: sxmwch@sdu.edu.cn

[b]College of Biological and Environmental Engineering, Binzhou University, Binzhou 256600, China

[c]Center for Optics Research and Engineering (CORE), Shandong University, Qingdao 266237, China. E-mail: lzq@sdu.edu.cn

order to understand the influence of different aldehydes for the reactions, we also discussed the reaction between CH_3CHO and HSO_3^- or SO_3^{2-}. Besides, the total rate constant (k_{total}, M^{-1} s^{-1}) for the individual reaction pathway within the range of 200 to 298 K were calculated. The further oxidation of the reaction products ($CH_2(OH)SO_3^-$ and $CH_3CH_2(OH)SO_3^-$) by OH radical and O_2 also be talked about.

Computational methods

The Gaussian-09 suite of programs was used to perform all the quantum chemistry calculations described in this paper. The density functional theory (DFT) was used for calculations.[18] All the geometrical structures (including reactants, pre-reactive complexes, transition states and products) calculated in this paper were optimized using the M06-2X functional at the 6-311++G(d,p) basis set.[19,20] Vibrational frequencies were calculated at the same level of theory to ascertain the local minimum points and the transition states, which supposed to have zero and one imaginary frequency. We also performed intrinsic reaction coordinate (IRC)[21] calculations in order to prove whether the transition state we found were the correct. Single-point energies were refined using the CCSD(T) method[22] with the aug-cc-pVTZ basis set.[23–25] Very recently, many high level quantum chemical methods have been used for the atmosphere reactions in order to obtain more reliable and excellent intrinsic accuracy.[26–28] In this article, under the consider of computational speed and accuracy, we think the dual-level strategy (CCSD(T)/aug-cc-pVTZ//M06-2X/6-311++G(d, p) level of theory) is appropriate. M06-2X functional has been widely used in theoretical calculation and can be better for ionic hydrogen-bonding interactions and identifying the global minimum conformer.[29–36] Been considered as the "gold standard" of quantum chemistry, CCSD(T) method was widely been used for reactions of organic matters and has high level accuracy. Thus we choose M06-2X functional at the 6-311++G(d,p) basis set for geometrical structures optimization and CCSD(T) method with the aug-cc-pVTZ basis set for single point energy calculation in this paper.[22,37–40] The Gibbs free energies were calculated by the following equation: $G = E$ (single-point energy) + G_{corr} (thermal correction to Gibbs free energy). The geometries were drawn using the CYLview software package.[41]

For the kinetics analysis, the conventional transition-state theory (TST)[42] with Wigner tunneling correction was used to calculate the rate constants. All rate constants were calculated by using the KiSThelP program.[43]

Results and discussion

Reaction of HCHO with dissolved SO_2

It aqueous phase, dissolved SO_2 can be dissociated to form HSO_3^- and SO_3^{2-}. Thus, we focus on the reactions of HSO_3^- + HCHO and SO_3^{2-} + HCHO.

As shown in Fig. 1(a), when HCHO approaches HSO_3^-, the reaction occurs via a five-membered cyclic prereactive complex HCHO···HSO_3^- (C1). C1 is regarded as the initial step of the HCHO and HSO_3^- reaction because C1 is connected with the

transition state TS1. The C1 is held together through a hydrogen bond and an electron donor–acceptor type of interaction between the two molecules. The change of the distances of C_b··· O_d and S_c···Ce are all shorten from 2.11 Å (C1) to 1.70 Å (TS1) and 3.24 Å (C1) to 2.11 Å (TS1), respectively. The reaction proceeds via a transition state TS1 with a barrier of 9.7 kcal mol^{-1} to produce $CH_2(OH)SO_3^-$ (HMS).

When SO_3^{2-} reacts with HCHO, the process is similar with the HCHO + HSO_3^- reaction. From Fig. 1(b), it can be found that the free energy of the complex C2 is 22.5 kcal mol^{-1} lower than reactants. Similar with C1, C2 is regarded as the initial step of the HCHO and SO_3^{2-} reaction. The complex C2 is held together by one van der Waals interaction. The change of distance between S_a···C_b is from 2.91 Å to 2.67 Å. The result is contrary to that of the HCHO + HSO_3^-, in which the higher free energy of the C1 can be observed. Once the C2 is formed, it can easily transform to product $CH_2(O^-)SO_3^-$ because the free energy of transition state TS2 is only 1.6 kcal mol^{-1} higher than the complex C2.

According to the analysis above, it is clear that the SO_3^{2-} is more likely to react with HCHO. However, the dissolved SO_2 exist in the form of HSO_3^- in the pH range of 2–7,[44] and the acidic condition of aerosol particles can be found in Beijing winter haze.[45] Thus, the HSO_3^- predominates in aerosol particles of Beijing winter haze so as to that the main reaction is HCHO + HSO_3^- in these aerosol particles. And only the further oxidation of HMS will be discussed in the latter part.

Reaction of CH_3CHO with dissolved SO_2

In order to study the effect of different aldehydes on the reaction, we also discussed the reaction between CH_3CHO with dissolved SO_2. As shown in Fig. 2(a), CH_3CHO + HSO_3^- reaction is firstly considered. The reaction is initiated with the formation of a five-ringlike structure complex CH_3CHO···HSO_3^- (C3), followed by the formation of a transition state TS3 to produce $CH_3CH(OH)$ SO_3^- (HES). The complex C3 is held together by one hydrogen bond and one van der Waals interaction. As shown in Fig. 2(a), the hydrogen atom (H_b) of HSO_3^- interacts with the oxygen atom (O_d) of CH_3CHO to form one hydrogen bond, and the sulfur atom (S_c) of HSO_3^- reacts with the carbon atom (C_e) of CH_3CHO. It is obviously that the distances between S_c···C_e and H_b···O_d are all shorten. The barrier in this reaction is 16.6 kcal mol^{-1}, which is larger than that of HCHO + HSO_3^- reaction.

For CH_3CHO + SO_3^{2-} reaction in Fig. 2(b), the formed complex C4 is also lower in energy than the reactants, which is similar with the HCHO + SO_3^{2-} reaction. The product CH_3-$CH(O^-)SO_3^-$ can be produced from the C4. The complex C4 is held together by one van der Waals interaction. As shown in Fig. 2(b), and sulfur atom (S_a) is involved in the formation of van der Waals interaction with a carbon atom (C_b) of HSO_3^-. The distance between S_a and C_b changes from 3.30 Å (C4) to 2.49 Å (TS4). The process needs to cross a transition state TS4 and to overcome the barrier of 2.5 kcal mol^{-1}, which is higher than that in HCHO + SO_3^{2-} reaction.

On the basis of the results, it can be concluded that the reactivity of HCHO with dissolved SO_2 is higher than that of another aldehydes with dissolved SO_2.
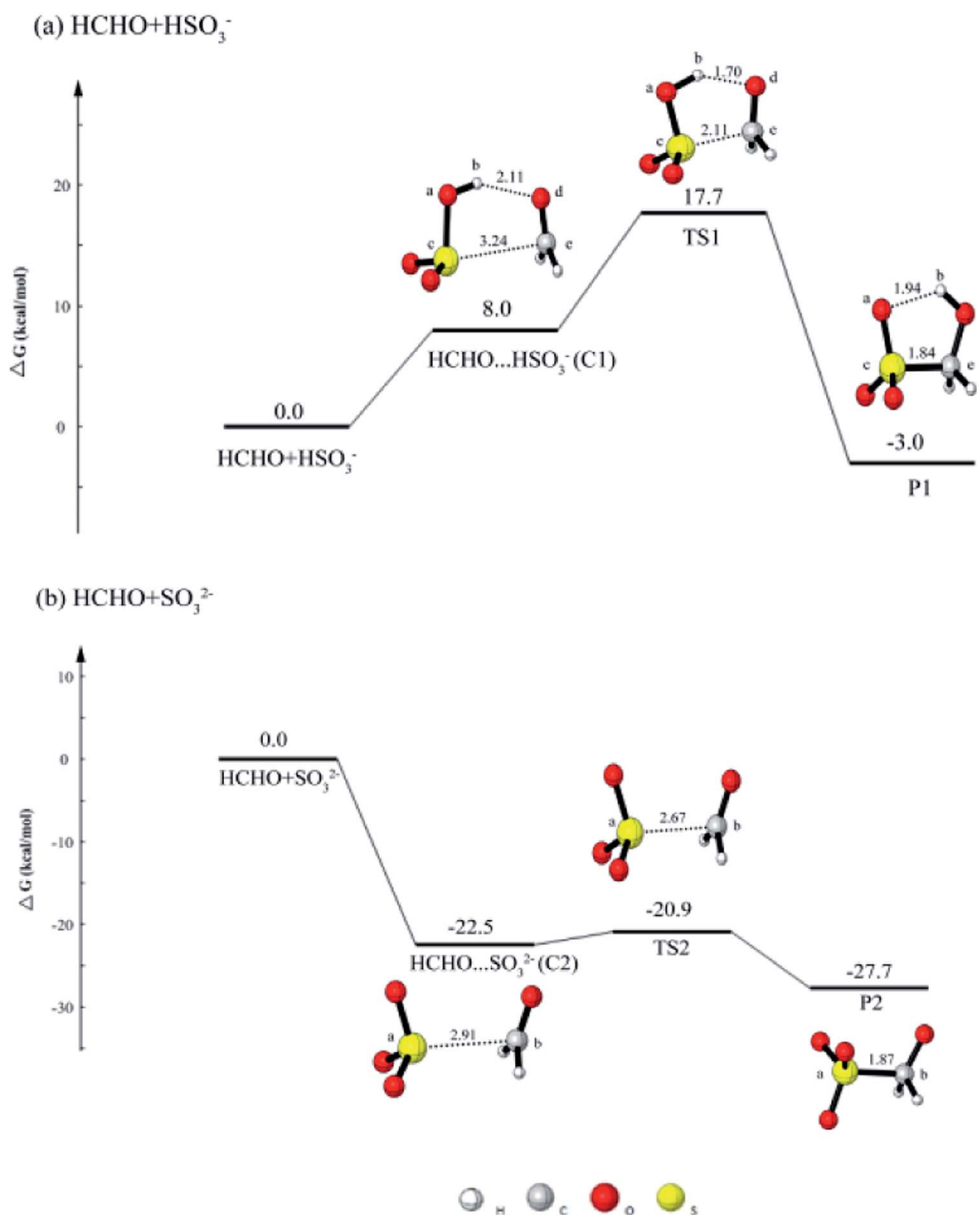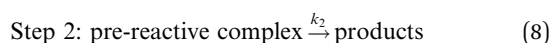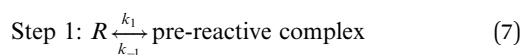
Fig. 1 The calculated free energy diagram for (a) the HCHO + HSO_3^- reaction, and for (b) the HCHO + SO_3^{2-} reaction calculated at the CCSD(T)/aug-cc-pVTZ//M06-2X/6-311++G(d, p) level of theory.

Rate calculation

In terms of the theoretical results discussed above, the reactions occur through a two-step mechanism, involving firstly a fast pre-equilibrium between the reactants and a pre-reactive complex, and the irreversible formation of the products, which can be characterized by eqn (7) and (8).

$$\text{Step 1: } R \underset{k_{-1}}{\overset{k_1}{\longleftrightarrow}} \text{pre-reactive complex} \tag{7}$$

$$\text{Step 2: pre-reactive complex} \overset{k_2}{\rightarrow} \text{products} \tag{8}$$

In the above reactions, k_1 is the kinetic rate constant characterizing the forward bimolecular reaction step (in cm³ per molecule per s), whereas k_{-1} and k_2 represent the backward and

forward unimolecular reaction rate constants (in s^{-1}). A steady-state analysis of the total reaction pathway's rate constant is formulated as:

$$k_{\text{total}} = \frac{k_1 k_2}{k_{-1} + k_2} = k_{\text{eq}} k_2 \tag{9}$$

And K_{eq} and k_2 are the equilibrium constant of the first step and the rate constant of the second step in the reactions, respectively. The computed data are shown in Table 1.

The rate constants of HCHO + SO_3^{2-} are ~10^9 to 10^7 times than that of HCHO + HSO_3^-, whereas rate constants of CH_3CHO + SO_3^{2-} is 8–6 orders of magnitude larger than that of CH_3CHO + HSO_3^- within range of 200–298 K. These results show that the reaction between aldehydes and SO_3^{2-} is faster, which is consistent with the analysis above. For HCHO and CH_3CHO, it
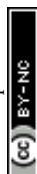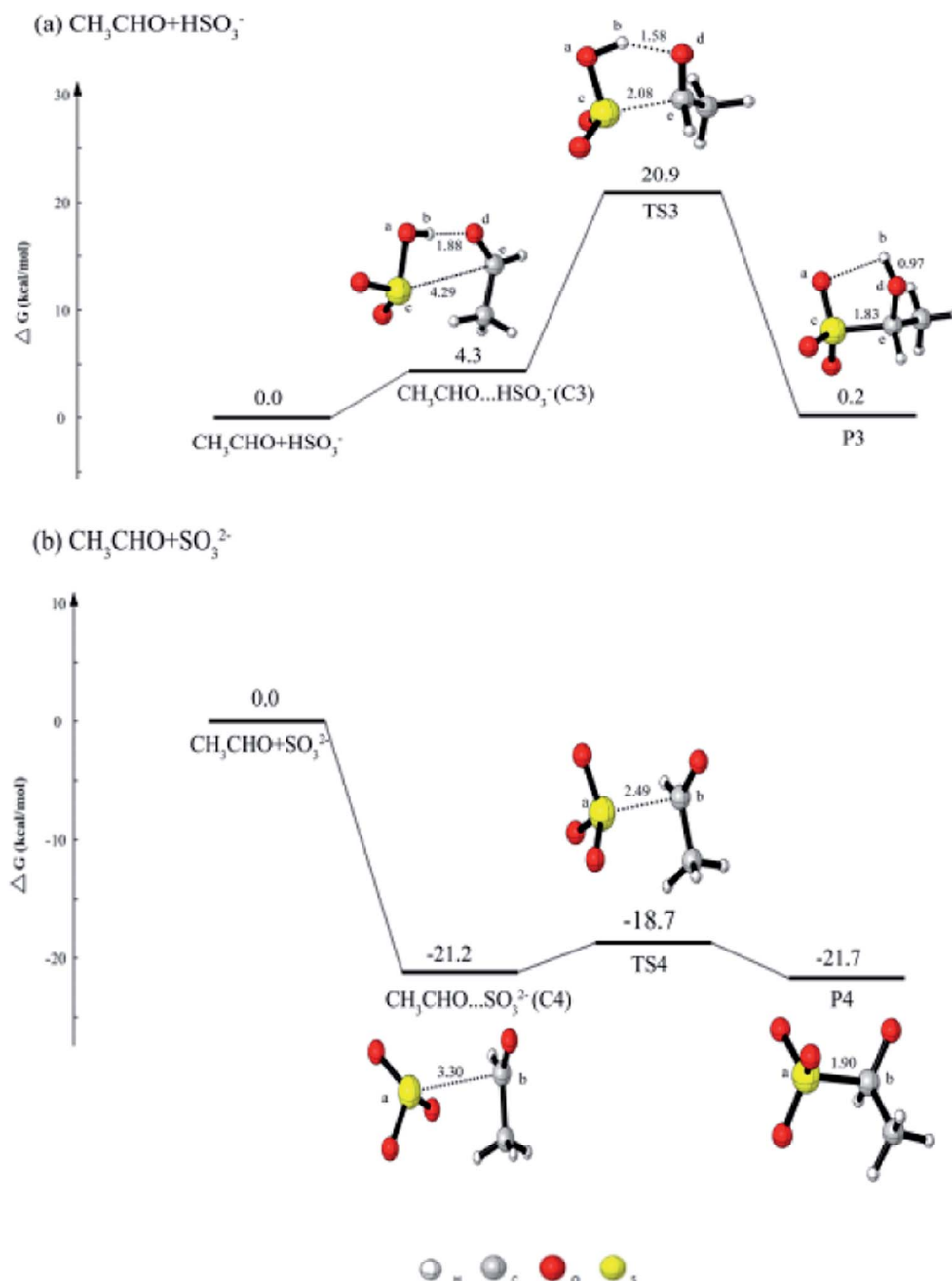
Fig. 2 The calculated free energy diagram for (a) the $CH_3CHO + HSO_3^-$ reaction, and for (b) the $CH_3CHO + SO_3^{2-}$ reaction calculated at the CCSD(*T*)/aug-*cc*-pVTZ//M06-2X/6-311++G(d, p) level of theory.

is clear that the rate constants between HCHO and HSO_3^- or SO_3^{2-} are larger than that between CH_3CHO and HSO_3^- or SO_3^{2-}, which is coincident with the discussion above.

Although the reaction between aldehydes and SO_3^{2-} is faster, HSO_3^- is the main form of dissolved SO_2 in the aerosol particles, leading to that the reaction of aldehydes with HSO_3^-

Table 1 The total rate constant (k_{total}, M^{-1} s^{-1}) for the individual reaction pathway within the temperature range from 200 to 298 K

	200 K	220 K	240 K	260 K	280 K	298 K
$HCHO + HSO_3^- \rightarrow CH_2(OH)SO_3^-$	4.00×10^{-3}	1.70×10^{-2}	6.06×10^{-2}	1.73×10^{-1}	4.27×10^{-1}	8.60×10^{-1}
$HCHO + SO_3^{2-} \rightarrow CH_2(O^-)SO_3^-$	3.21×10^6	2.74×10^6	2.42×10^6	2.20×10^6	2.04×10^6	1.93×10^6
$CH_3CHO + HSO_3 \rightarrow CH_3CH(OH)SO_3^-$	3.52×10^{-6}	2.41×10^{-5}	1.20×10^{-4}	4.69×10^{-4}	1.52×10^{-3}	3.80×10^{-3}
$CH_3CHO + SO_3^{2-} \rightarrow CH_3CH(O^-)SO_3^-$	3.96×10^2	5.85×10^2	8.23×10^2	1.10×10^3	1.43×10^3	1.76×10^3

predominates in the aqueous phase of aerosol particles. Thus, in the next part, only $CH_2(OH)SO_3^-$ and $CH_3CH(OH)SO_3^-$ will be talked about.

Oxidation of HMS and HES

As the oxidation of HMS is of great importance, it is meaningful and necessary to investigate the oxidation mechanism. Previous research[46] has investigated the oxidation of HMS with H_2O_2 and O_3, there was no calculation on the oxidation by OH radical. Thus, we will calculate the HMS + OH reaction so as to confirm whether peroxysulfate radicals ($SO_5^{\cdot-}$) can be produced.

Fig. 3(a) shows the potential energy profile for $CH_2(OH)SO_3^-$ + OH reaction. In the reaction process, HMS firstly reacts with OH radical to form the complex $CH_2(OH)SO_3^-\cdots OH$ (C5) with the free energy release of 35.2 kcal mol^{-1}. The C5 can evolve via TS5 with a barrier of 29.9 kcal mol^{-1} into $CH_2(OH)_2$ and $SO_3^{\cdot-}$. The $SO_3^{\cdot-}$ can continue to react with O_2 to produce $SO_5^{\cdot-}$. The addition reaction between $SO_3^{\cdot-}$ and O_2 can occur via a transition state TS6 with the barrier of 12.2 kcal mol^{-1}.

The further oxidation mechanism of $CH_3CH(OH)SO_3^-$ (HES) by OH radical is similar with that of HMS by OH radical. As can be seen from Fig. 3(b), OH radical is added to HES to produce the complex $CH_3CH(OH)SO_3^-\cdots OH$ (C6). The reaction proceeds via a transition state TS7 with a barrier of 31.0 kcal mol^{-1}. The formed $SO_3^{\cdot-}$ in this reaction also react with O_2 to form $SO_5^{\cdot-}$, and the process has the same barrier of 12.2 kcal mol^{-1}.
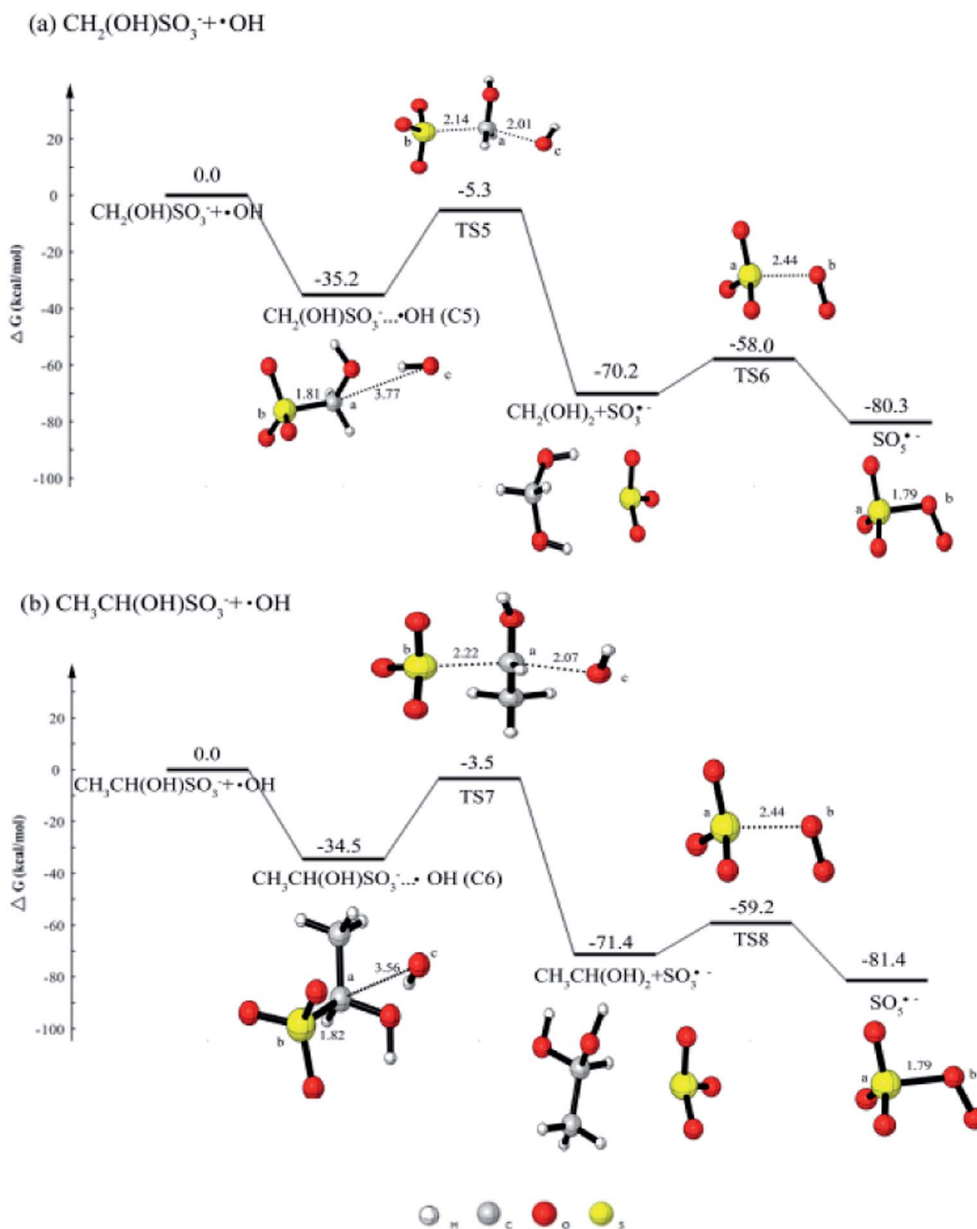

Fig. 3 The calculated free energy diagram for (a) the $CH_2(OH)SO_3^-$ + ·OH reaction, and for (b) the $CH_3CH(OH)SO_3^-$ + ·OH reaction calculated at the CCSD(T)/aug-cc-pVTZ//M06-2X/6-311++G(d, p) level of theory.

Conclusions

HMS is the major OS species. In this paper, we investigated the formation of HMS using the quantum chemical calculations. Besides, other aldehydes like acetaldehyde also exist in the atmosphere. The similar structure between formaldehyde and acetaldehyde makes us to think the effect of different aldehydes on their reaction with dissolved SO_2. Thus, the reaction between acetaldehyde and dissolved SO_2 also was discussed.

The result shows that the energy barrier for $CH_3CHO + HSO_3^-$ reaction is 16.6 kcal mol^{-1}, which is a little higher than 9.7 kcal mol^{-1} for reaction of HCHO with HSO_3^-. The barrier (2.5 kcal mol^{-1}) of $CH_3CHO + SO_3^{2-}$ reaction is larger than that (1.6 kcal mol^{-1}) of HCHO and SO_3^{2-} reaction. These results indicate that the reaction of aldehydes with SO_3^{2-} is easier than that with HSO_3^-. However, the HSO_3^- is the main form of dissolved SO_2 in the aerosol particles, leading to that the aldehydes + HSO_3^- reaction dominates. Thus, the main products are $CH_2(OH)SO_3^-$ and $CH_3CH(OH)SO_3^-$. Their further oxidation by OH radical and O_2 shows that the $SO_3^{\cdot-}$ and $SO_5^{\cdot-}$ radical can be formed.

Conflicts of interest

There are no conflicts to declare.

Acknowledgements

Notes and references

1 D. J. Eatough and L. D. Hansen, *Sci. Total Environ.*, 1984, **36**, 319–328.

2 R. W. Dixon and H. Aasen, *Atmos. Environ.*, 1999, **33**, 2023–2029.

3 J. D. Surratt, J. H. Kroll, T. E. Kleindienst, E. O. Edney, M. Claeys, A. Sorooshian, N. L. Ng, J. H. Offenberg, M. Lewandowski, M. Jaoui, R. C. Flagan and J. H. Seinfeld, *Environ. Sci. Technol.*, 2007, **41**, 517–527.

4 Y. Iinuma, C. Müller, T. Berndt, O. Böge, M. Claeys and H. Herrmann, *Environ. Sci. Technol.*, 2007, **41**, 6678–6683.

5 J. D. Blando, R. J. Porcja, T.-H. Li, D. Bowman, P. J. Lioy and B. J. Turpin, *Environ. Sci. Technol.*, 1998, **32**, 604–613.

6 M. P. Tolocka and B. Turpin, *Environ. Sci. Technol.*, 2012, **46**, 7978–7983.

7 R. J. Charlson, J. E. Lovelock, M. O. Andreae and S. G. Warren, *Nature*, 1987, **326**, 655–661.

8 M. Claeys, W. Wang, R. Vermeylen, I. Kourtchev, X. Chi, Y. Farhat, J. D. Surratt, Y. Gómez-González, J. Sciare and W. Maenhaut, *J. Aerosol Sci.*, 2010, **41**, 13–22.

9 J. Liao, K. D. Froyd, D. M. Murphy, F. N. Keutsch, G. Yu, P. O. Wennberg, J. M. St. Clair, J. D. Crounse, A. Wisthaler, T. Mikoviny, J. L. Jimenez, P. Campuzano-Jost, D. A. Day, W. Hu, T. B. Ryerson, I. B. Pollack, J. Peischl, B. E. Anderson, L. D. Ziemba, D. R. Blake, S. Meinardi and G. Diskin, *J. Geophys. Res.: Atmos.*, 2015, **120**, 2990–3005.

10 D. D. Huang, Y. J. Li, B. P. Lee and C. K. Chan, *Environ. Sci. Technol.*, 2015, **49**, 3672–3679.

11 T. M. Olson and M. R. Hoffmann, *Atmos. Environ.*, 1989, **23**, 985–997.

12 S. Song, M. Gao, W. Xu, Y. Sun, D. R. Worsnop, J. T. Jayne, Y. Zhang, L. Zhu, M. Li, Z. Zhou, C. Cheng, Y. Lv, Y. Wang, W. Peng, X. Xu, N. Lin, Y. Wang, S. Wang, J. W. Munger, D. J. Jacob and M. B. McElroy, *Atmos. Chem. Phys.*, 2019, **19**, 1357–1371.

13 C. Wagner, *Ber. Dtsch. Chem. Ges.*, 1929, **62**, 2873–2877.

14 P. Jones and K. Oldham, *The theory of the formaldehyde clock reaction*, 1963.

15 P. Bell Ronald and P. G. Evans, *Proc. R. Soc. London, Ser. A*, 1966, **291**, 297–323.

16 S. D. Boyce and M. R. Hoffmann, *J. Phys. Chem.*, 1984, **88**, 4740–4746.

17 J. W. Munger, D. J. Jacob, J. M. Waldman and M. R. Hoffmann, *J. Geophys. Res.*, 1983, **88**, 5109–5121.

18 L. Vereecken and J. S. Francisco, *Chem. Soc. Rev.*, 2012, **41**, 6259–6293.

19 Y. Zhao and D. G. Truhlar, *Theor. Chem. Acc.*, 2008, **120**, 215–241.

20 R. Krishnan, J. S. Binkley, R. Seeger and J. A. Pople, *J. Chem. Phys.*, 1980, **72**, 650–654.

21 K. Fukui, in *Frontier Orbitals and Reaction Paths*, World Scientific, 1997, vol. 7, pp. 471–476.

22 G. D. Purvis and R. J. Bartlett, *J. Chem. Phys.*, 1982, **76**, 1910–1918.

23 A. K. Wilson, T. van Mourik and T. H. Dunning, *J. Mol. Struct.: THEOCHEM*, 1996, **388**, 339–349.

24 J. A. Pople, M. Head-Gordon and K. Raghavachari, *J. Chem. Phys.*, 1987, **87**, 5968–5975.

25 A. Godfrey-Kittle and M. Cafiero, *Int. J. Quantum Chem.*, 2006, **106**, 2035–2043.

26 B. Long, J. L. Bao and D. G. Truhlar, *J. Am. Chem. Soc.*, 2016, **138**, 14409–14422.

27 B. Long, J. L. Bao and D. G. Truhlar, *Proc. Natl. Acad. Sci. U. S. A.*, 2018, **115**, 6135–6140.

28 B. Long, J. L. Bao and D. G. Truhlar, *J. Am. Chem. Soc.*, 2019, **141**, 611–617.

29 M. Walker, A. J. A. Harvey, A. Sen and C. E. H. Dessent, *J. Phys. Chem. A*, 2013, **117**, 12590–12600.

30 D. S. Huh and S. J. Choe, *J. Porphyrins Phthalocyanines*, 2010, **14**, 592–604.

31 H. A. Rypkema, A. Sinha and J. S. Francisco, *J. Phys. Chem. A*, 2015, **119**, 4581–4588.

32 B. Long, X.-F. Tan, C.-R. Chang, W.-X. Zhao, Z.-W. Long, D.-S. Ren and W.-J. Zhang, *J. Phys. Chem. A*, 2013, **117**, 5106–5116.

33 S. Pari, I. A. Wang, H. Liu and B. M. Wong, *Environ. Sci.: Processes Impacts*, 2017, **19**, 395–404.

34 X. Shi, R. Zhang, Y. Sun, F. Xu, Q. Zhang and W. Wang, *Phys. Chem. Chem. Phys.*, 2018, **20**, 1005–1011.

35 N. Rashidian, E. Zahedi and A. Shiroudi, *Sci. Total Environ.*, 2019, **679**, 106–114.

36 A. S. M. Gad El-Hak, A. A. K. Mohammed, A. F. Abdel Hakiem and R. M. Mahfouz, *Spectrochim. Acta, Part A*, 2019, **222**, 117200.

37 G. Knizia, T. B. Adler and H.-J. Werner, *J. Chem. Phys.*, 2009, **130**, 054104.

38 P. R. Nagy, G. Samu and M. Kállay, *J. Chem. Theory Comput.*, 2018, **14**, 4193–4215.

39 M. B. Oviedo, N. V. Ilawe and B. M. Wong, *J. Chem. Theory Comput.*, 2016, **12**, 3593–3602.

40 J. Řezáč and P. Hobza, *Chem. Rev.*, 2016, **116**, 5038–5071.

41 C. Y. Legault, *CYLview 1.0 b*, Université de Sherbrooke, 2009, http://www.cylview.org.

42 D. G. Truhlar, B. C. Garrett and S. J. Klippenstein, *J. Phys. Chem.*, 1996, **100**, 12771–12800.

43 S. Canneaux, F. Bohr and E. Henon, *J. Comput. Chem.*, 2014, **35**, 82–93.

44 R. Zhang, G. Wang, S. Guo, M. L. Zamora, Q. Ying, Y. Lin, W. Wang, M. Hu and Y. Wang, *Chem. Rev.*, 2015, **115**, 3803–3855.

45 S. Song, M. Gao, W. Xu, J. Shao, G. Shi, S. Wang, Y. Wang, Y. Sun and M. B. McElroy, *Atmos. Chem. Phys.*, 2018, **18**, 7423–7438.

46 J. W. Munger, C. Tiller and M. R. Hoffmann, *Science*, 1986, **231**, 247.

This journal is © The Royal Society of Chemistry 2019